Heliyon 10 (2024) e33794

Contents lists available at ScienceDirect

Heliyon

journal homepage: www.cell.com/heliyon

Research article

Ferroptosis-related gene signature and clinical prognostic factors as prognostic marker for colon adenocarcinoma

Qunzhang Zeng [a,1], Lin Han [b,1], Qiuxia Hong [c], Guan-Cong Wang [a], Xia-Juan Xue [a], Yicong Fang [a,*], Jing Liu [d,**]

[a] Department of Colorectal and Anal Surgery, Zhangzhou Affiliated Hospital of Fujian Medical University, Zhangzhou, Fujian, 363000, China
[b] Department of Gastroenterology, Zhangzhou Affiliated Hospital of Fujian Medical University, Zhangzhou, Fujian, 363000, China
[c] Medical Department, Zhangzhou Affiliated Hospital of Fujian Medical University, Zhangzhou, Fujian, 363000, China
[d] Smartquerier Gene Technology (Shanghai) Co., Ltd., Shanghai, 201203, China

ARTICLE INFO

Keywords:
Ferroptosis
Colon adenocarcinoma
Ferroptosis score
Prognostic model

ABSTRACT

Aim: To build a ferroptosis-related prognostic model for patients with colon adenocarcinoma (COAD).

Methods: COAD expression profiles from The Cancer Genome Atlas were used as the training set and GSE39582 from Gene Expression Omnibus as the validation set. Differentially expressed ferroptosis-related genes between patients with COAD and normal controls were screened, followed by tumor subtype exploration based on ferroptosis-related gene expression levels. A ferroptosis score (FS) model was constructed using least absolute shrinkage and selection operator penalized Cox analysis. Based on FS, patients were subgrouped into high- and low-risk subgroups and overall survival was predicted. The potential prognostic value of the FS model and the clinical characteristics were investigated using receiver operating characteristic curves.

Results: Twenty-four differentially expressed ferroptosis-related genes were identified, four of which (*CYBB*, *PRNP*, *ACSL4*, and *ACSL6*) were included in the prognostic signature. Moreover, age, pathological T stage, and tumor recurrence were independent prognostic factors for COAD. The FS model combined with three independent prognostic factors showed the best prognostic value (The Cancer Genome Atlas: area under the curve = 0.897; GSE39582: area under the curve = 0.858).

Conclusion: The novel prognostic model for patients with COAD constructed by pairing the FS model with three important independent prognostic factors showed promising clinical predictive value.

1. Introduction

Colon cancer is one of the most common malignant tumors in both men and women worldwide and is also accepted as a leading

* Corresponding author.Department of Colorectal and Anal Surgery, Zhangzhou Affiliated Hospital of Fujian Medical University, No. 59, Shengli West Road, Xiangcheng District, Zhangzhou City, Fujian Province, 363000, China.
** Corresponding author. Smartquerier Gene Technology (Shanghai) Co., Ltd., Huahong Innovation Park, Shenjiang Road, Pudong New Area, Shanghai, 201203, China.
E-mail addresses: 13806909328@163.com (Y. Fang), Aaronbio@163.com (J. Liu).
[1] Co-first authors: Qunzhang Zeng and Lin Han.

https://doi.org/10.1016/j.heliyon.2024.e33794
Received 11 September 2023; Received in revised form 25 June 2024; Accepted 26 June 2024
Available online 28 June 2024

cause of cancer-related deaths in China [1,2]. In general, according to the pathologic classification, 80%–90 % of colon cancer cases are diagnosed with colon adenocarcinoma (COAD) [3]. Among them, 25 % of patients with COAD have unresectable metastatic disease [4], and these patients have a significantly shorter 5-year overall survival (OS) rate (12.5 %) as compared with that in patients having local stage disease (90.3 %) [5]. Thus, exploring robust and promising predictive signatures for estimating clinical outcomes would be of great clinical significance for COAD cancers.

Ferroptosis, first proposed in 2012 by Dixon et al. [6], is a phenomenon of regulated cell death characterized by lipid peroxidation and iron-dependent accumulation of intracellular reactive oxygen species. It differs from other forms of cell death, such as autophagy and apoptosis [7]. Further increasing evidence reveals that ferroptosis is critical in metabolism, cell death, and redox biology [8]. With the accumulation of knowledge regarding ferroptosis, ferroptosis-induced cell death has gradually been demonstrated as a novel biomarker for treating cancers, particularly in patients resistant to traditional therapies [9]. The predictive and prognostic values of ferroptosis-related prognostic signatures have been proposed. For example, Tang and his colleagues established a 25 differentially expressed ferroptosis-related lncRNAs prognostic signature of head and neck squamous cell carcinoma [10]. Xu et al. showed that colorectal cancer was sensitive to ferroptosis mediated by modulating SLC7A11 [11]. Similarly, Park and his colleagues demonstrated that Kras-mutant colorectal cancer cells could be inhibited by modulating the ferroptosis activation [12]. Recently, Xin et al. confirmed that ferroptosis-related gene signature was beneficial for predicting individualized prognosis [13]. For patients with COAD, there is no ideal tool for predicting survival situation.

Therefore, to provide a new strategy for the management of clinical treatment, we developed a novel ferroptosis-related gene signature as a prognostic model for COAD by investigating clinical information and transcriptome profiles of publicly available datasets. First, publicly available data for COAD were downloaded, and differentially expressed ferroptosis-related genes (DEFGs) were screened. A ferroptosis score (FS) model was also constructed. The participants were then grouped into low- and high-risk groups. We constructed prognostic models based on the ferroptosis-related genes and clinical prognostic factors. Finally, a novel prognostic model based on the FS model and three important independent clinical factors was established, and its clinical prediction value in COAD was evaluated.

2. Materials and methods

2.1. Collection of transcriptome data and processing

The expression profiles of the training dataset of COAD, as well as clinical information, were screened from the database of The Cancer Genome Atlas (TCGA), and these data were obtained using the Illumina HiSeq 2000 detection platform. Of the 512 samples, 479, including 41 controls and 438 COAD samples, provided clinical information.

The validation dataset was searched using the National Center for Biotechnology Information Gene Expression Omnibus [14]. The data set met the following criteria: 1) the studied sample was COAD tumor tissue; 2) more than 200 COAD samples were involved in the dataset; 3) clinical prognostic information was provided in the study. Finally, GSE39582 was identified using the GeneChip GPL570 Affymetrix Human Genome U133 Plus 2.0 Array and enrolled [15]. The data set contained 585 samples. Among these, 519 COAD tumor samples had clinical survival prognostic information.

2.2. Exploration of DEFGs

Ferroptosis-related genes were screened from previously published literature and the GSEA MSigDB database [16] and the genes were combined as a list of ferroptosis-related genes. Furthermore, the expression levels of these genes in the TCGA database were extracted, and DEFGs between the COAD and normal groups were identified using the between-group *t*-test in R language 3.6.1. $P < 0.05$ was defined as significant difference. Hierarchical cluster analysis was then performed using pheatmap Version 1.0.8 in R3.6.1 [17].

2.3. Analysis of sample subtypes

The sample subtypes were analyzed based on ferroptosis-related gene levels using the ConsensusClusterPlus package in R3.6.1 (Version 1.54.0) [18]. Subsequently, the survival package in the R3.6.1 language (Version 2.41–1) was used to evaluate the survival prognosis correlation between subtypes [19]. Afterwards, we analyzed clinical characteristics of individuals involved in each subtype group.

2.4. Establishment of a prognostic model for COAD based on DEFGs

2.4.1. Screen of optimal combination of ferroptosis-related genes and construction of FS model

The least absolute shrinkage and selection operator (LASSO) is a tool for improving both interpretation and prediction accuracy based on high-dimensional data analysis [20]. By using LASSO, survival regression analysis was designed to screen the optimal combination of ferroptosis-related genes.

The FS model was further constructed using the LASSO prognostic coefficient to optimize the combination of DEFGs and target gene expression levels in TCGA training set as follows:

$$FS = \sum Coef_{genes} \times Exp_{genes}$$

Here, $Coef_{genes}$ represents the target gene LASSO prognostic coefficient, and Exp_{genes} represents the target gene levels in TCGA training dataset.

2.4.2. The effectiveness of FS survival prognosis prediction model

The FS values of the DEFGs involved in the verification and training sets were calculated. Subsequently, we divided the samples into high- and low-risk groups stratified by median FS value. Furthermore, Kaplan–Meier curves were constructed to evaluate the OS of the high- and low-risk groups using the survival package (Version 2.41–1) in R3.6.1 [19].

2.5. The association analysis between clinical factors and ferroptosis-related genes

2.5.1. Independent prognostic clinical factors

Based on clinical data from the TCGA training set and GSE39582 verification set, independent survival prognostic clinical factors associated with COAD were screened using multi-factor Cox and single factor regression analyses (survival package, Version 2.41–1) in the R3.6.1 language [19]. Log-rank $p < 0.05$ was set as the threshold to select clinical factors related to COAD survival performance, and Kaplan–Meier curve analysis was conducted to evaluate survival time under different clinical conditions [19].

The expression levels of the DEFGs involved in the model were compared between the different risk groups using the *t*-test in R 3.6.1.

2.6. Construction and comparison of multiple prognostic models

2.6.1. Comparison of DEFGs-based models

The survival status of the sample was predicted based on the prognostic value of each DEFG included in the model. The survival status of the samples was analyzed by comprehensively assessing the prognostic value of DEFGs in the FS model. Finally, the prognostic performances of the two values were compared using the area under the receiver operating characteristic (AUROC) curve.

The AUROC, as a quantitative ROC curve indicator, ranges from 0.5 to 1, and a value closer to 1 indicates better classifier performance. AUROC was calculated using pROC in R3.6.1 (Version 1.14.0, https://cran.r-project.org/web/packages/pROC/index.html) [21].

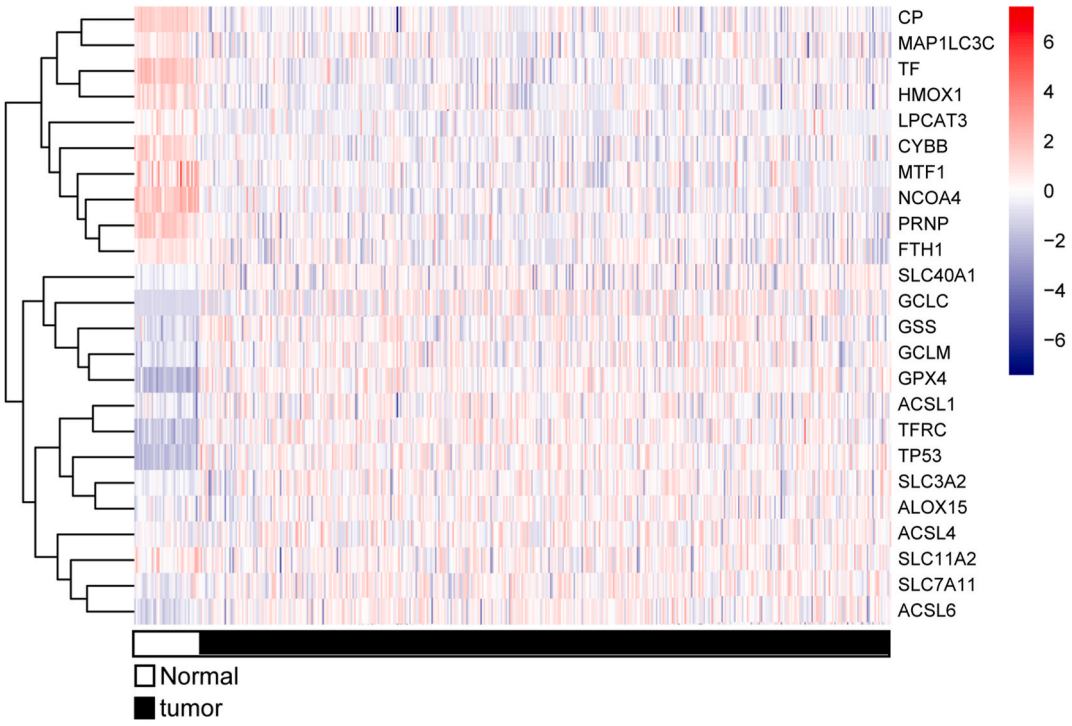

Fig. 1. The heatmap of ferroptosis-related genes with significantly different expression levels between colon adenocarcinoma and normal control samples.

2.6.2. Construction of a prognostic model according to independent prognostic-related clinical factors

The survival status of the individuals was first estimated based on the important independent prognostic-related clinical factors screened in the previous step, and then the survival status of the sample was comprehensively predicted by combining the aforementioned prognostic-related clinical factors. Finally, the prognostic performances of the two groups were compared.

2.6.3. Construction of a comprehensive model

A comprehensive prognostic model was constructed by combining important clinical factors based on the FS model and previous screening in the TCGA training set and the GSE39582 validation set. The performances of the models were then evaluated using the AUROC.

3. Results

3.1. Analysis of genes related to ferroptosis

In total, 24 DEFGs were identified. The cluster heat map of the DEFGs showed distinct gene expression trends in the normal and COAD samples (Fig. 1).

3.2. Subtype analysis based on DEFGs

Subtype analysis of COAD samples was performed based on the expression levels of the 24 DEFGs. Two different subtypes were identified: 223 and 215 COAD samples (Fig. 2A). Fig. 2B shows that a significant difference in survival was observed between the two subtypes. Furthermore, patients with subtype 1 had a better clinical survival prognosis than those with subtype 2.

Afterwards, the clinical information of the samples was compared (Table 1), and four clinical factors, including sex, death, pathologic M, and pathologic stage, were significantly different between the two subtypes, and their composition ratios in the two subtypes are shown in Fig. 3.

3.3. The prognostic model based on DEFGs

3.3.1. Screening of the optimal gene combination

The optimized gene combination was screened based on 24 DEFGs using the LASSO algorithm. Four optimized ferroptosis genes were identified: *CYBB*, *PRNP*, *ACSL4*, and *ACSL6*. The optimal combination for 1se was 0.03547.

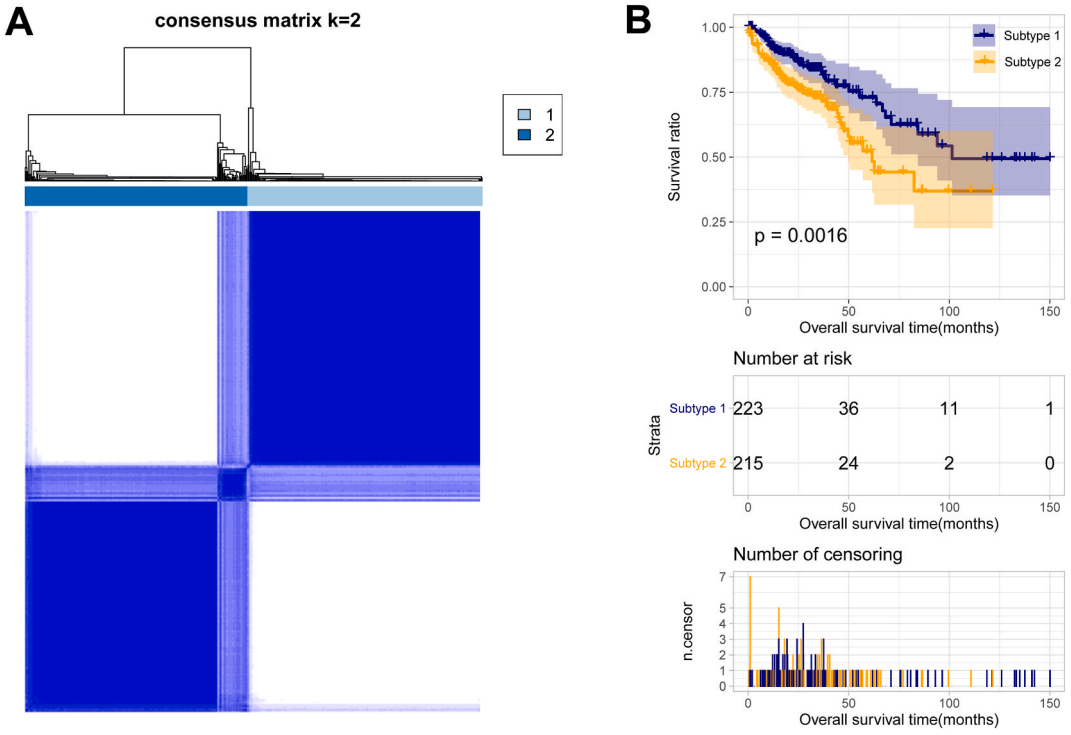

Fig. 2. Subgroup analysis and Kaplan–Meier curve analysis. A. Two subtypes were divided in the subtype analysis. B. Kaplan–Meier curve based on different subtypes.

Table 1
Clinical information comparison of samples from different subtype groups.

Characteristics total cases	Number (%)	Subtype		P-value
		Subtype 1 (N = 223)	Subtype 2 (N = 215)	
Age (years)				
≤60	134 (30.59)	66	68	6.79E-01
>60	304 (69.41)	157	147	
Sex				
Men	233 (53.2)	104	129	5.54E-03
Women	205 (46.8)	119	86	
Recurrence				
Yes	78 (17.81)	36	42	1.22E-01
No	293 (66.89)	159	134	
NA	67 (15.3)	28	39	
Dead				
Yes	101 (23.06)	41	60	2.30E-02
No	337 (76.94)	182	155	
Pathologic M				
0	325 (74.2)	177	148	1.22E-03
1	60 (13.7)	19	41	
NA	53 (12.1)	27	26	
Pathologic N				
0	257 (58.68)	132	125	5.19E-01
1	103 (23.52)	48	55	
2	78 (17.81)	43	35	
Pathologic T				
1	11 (2.51)	5	6	8.85E-01
2	76 (17.35)	36	40	
3	300 (68.49)	156	144	
4	51 (11.64)	26	25	
Pathologic Stage				
I	74 (16.89)	36	38	9.08E-03
II	168 (38.36)	90	78	
III	126 (28.77)	72	54	
IV	60 (13.7)	19	41	
NA	10 (2.28)	6	4	

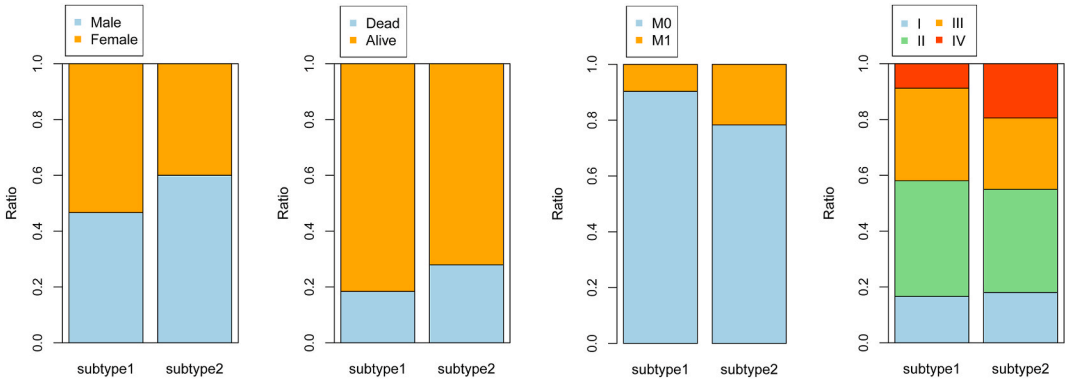

Fig. 3. Histogram of the composition ratio of different clinical factors in different subtypes.

Subsequently, according to the expression levels and LASSO regression coefficients of the four genes, FS was calculated as follows:

$$FS = (-0.0086728807) * ExpCYBB + (0.0068384710) * ExpPRNP + (-0.0004832706) * ExpACSL4 + (-0.0113962677) * ExpACSL6$$

3.3.2. FS value is related with survival prognosis

The distribution of the FS value, recurrence prognosis time distribution, and ROC curve of the high- and low-risk groups in the TCGA database and the validation database (GSE39582) were shown in Fig. 4A and B. Furthermore, the Kaplan–Meier curves of each dataset (TCGA and GSE39582) were constructed, and the results showed that the FS model prediction was significantly correlated with the actual prognosis in the high- and low-risk groups (Fig. 5A and B).

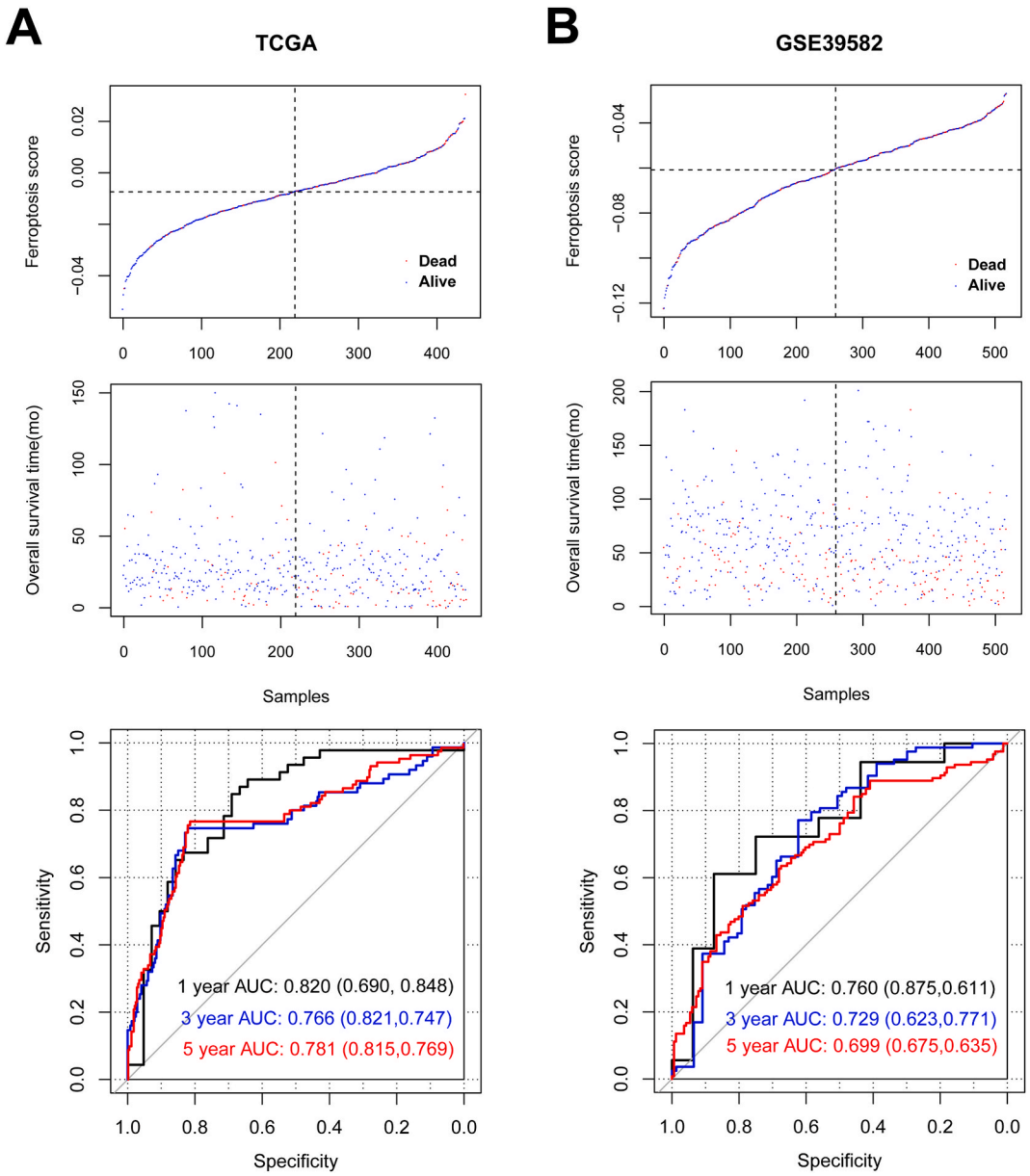

Fig. 4. Ferroptosis score distribution (above), survival time status (middle), and receiver operating characteristic curves of one, three, and five years according to prognostic characteristics of important genes (below) in TCGA training set and GSE39582 validation set. A: TCGA training set; B: GSE39582 validation set. TCGA, The Cancer Genome Atlas.

3.4. Screening of important clinical prognostic factors

Independent prognostic clinical factors were screened in both the validation and training datasets. As shown in Table 2, four factors, including age, pathologic T stage, tumor recurrence, and FS model status, were significantly independently related to prognosis.

Kaplan–Meier curves for age, pathologic T, and tumor recurrence in the TCGA training set and GSE39582 validation set are shown in Figs. 6 and 7, respectively. It was found that in the TCGA training set, the patients with age >60 years, higher pathologic T, and tumor recurrence were associated with poor OS (Fig. 6A, B, 6C), which were confirmed in the validation dataset (GSE39582) (Fig. 7A, B, 7C).

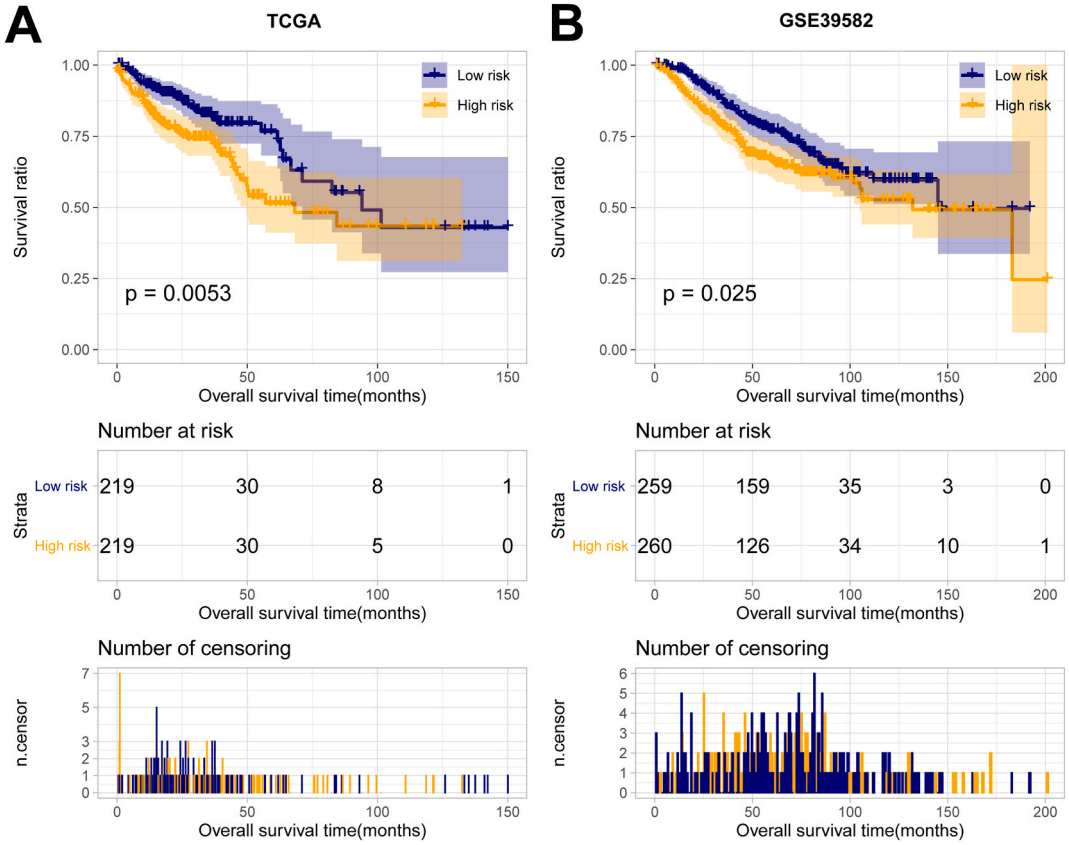

Fig. 5. Kaplan–Meier curve and prognosis in TCGA training set and GSE39582 validation set. A: TCGA training set; B: GSE39582 validation set. The green curve represents low-risk groups, and red curve represents high-risk group. The bottom figure shows the number of censored individuals who exit the risk set at time t, without an event. TCGA, The Cancer Genome Atlas.

Table 2
Screening of independent clinical prognosis factors.

Tables 2–1 Screening of independent clinical prognosis factors in The Cancer Genome Atlas.

Clinical characteristics	Univariable cox		Multivariable cox	
	HR (95 % CI)	P-value	HR (95 % CI)	P-value
Age (years, mean ± SD)	1.022 (1.005–1.039)	8.812E-03	1.039 (1.016–1.062)	7.430E-04
Sex (Men/Women)	1.101 (0.744–1.631)	6.299E-01	–	–
Pathologic M (M0/M1)	4.227 (2.687–6.648)	1.186E-11	1.461 (0.410–5.202)	5.584E-01
Pathologic N (N0/N1/N2)	1.990 (1.578–2.509)	1.226E-09	1.203 (0.683–2.120)	5.217E-01
Pathologic T (T1/T2/T3/T4)	2.424 (1.642–3.580)	4.762E-06	2.979 (1.609–5.515)	5.140E-04
Pathologic stage (I/II/III/IV)	2.060 (1.635–2.596)	2.891E-10	1.506 (0.579–3.922)	4.015E-01
Recurrence (Yes/No)	2.544 (1.625–3.981)	2.319E-05	1.881 (1.090–3.246)	2.317E-02
FS model status (High/Low)	1.756 (1.176–2.622)	5.209E-03	1.548 (0.931–2.574)	9.180E-03

Tables 2–2 Screening of independent clinical prognosis factors in GSE39582

Clinical characteristics	Uni-variable cox		Multi-variable cox	
	HR (95 % CI)	P-value	HR (95 % CI)	P-value
Age (years, mean ± SD)	1.035 (1.021–1.049)	5.985E-07	1.044 (1.028–1.060)	4.710E-08
Sex (Men/Women)	1.401 (1.017–1.930)	3.838E-02	1.216 (0.853–1.734)	2.803E-01
Pathologic M (M0/M1)	4.733 (2.827–7.925)	7.203E-11	7.147 (0.980–17.1369)	1.050E-01
Pathologic N (N0/N1/N2)	1.493 (1.220–1.827)	8.005E-05	1.643 (1.106–2.442)	1.400E-01
Pathologic T (T1/T2/T3/T4)	1.880 (1.393–2.538)	2.869E-05	1.536 (1.102–2.141)	1.130E-02
Pathologic stage (I/II/III/IV)	1.660 (1.305–2.111)	3.573E-05	0.530 (0.286–1.979)	4.290E-01
Recurrence (Yes/No)	5.931 (4.290–8.199)	2.000E-16	4.975 (3.463–7.145)	2.000E-16
FS model status (High/Low)	1.143 (1.045–1.961)	2.474E-02	1.148 (1.093–1.627)	4.394E-02

SD: standard deviation; FS, Ferroptosis score.

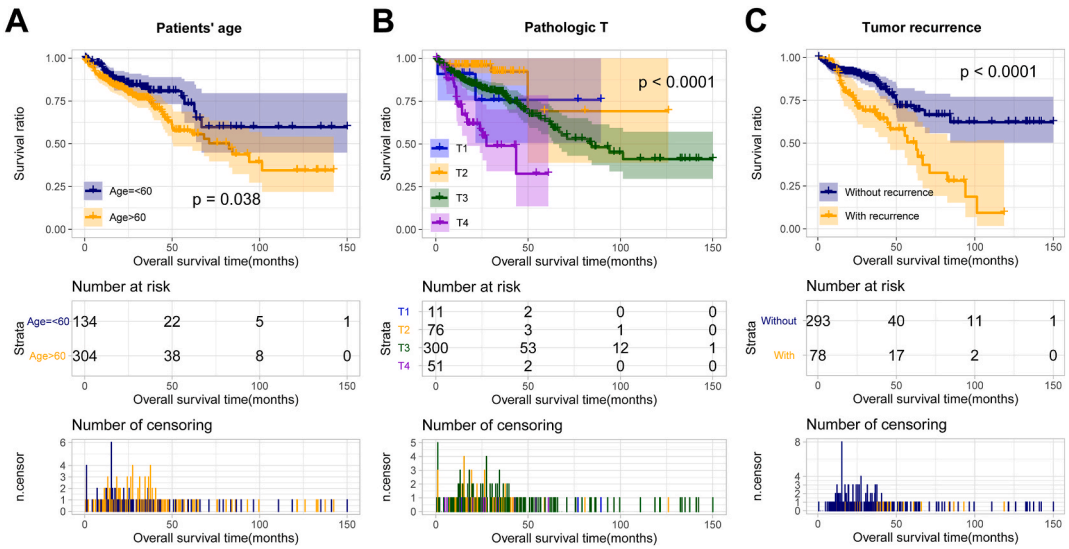

Fig. 6. Kaplan–Meier curve of age, pathologic T, and tumor recurrence in TCGA training set. A: age; B: pathologic T; C: tumor recurrence. TCGA, The Cancer Genome Atlas.

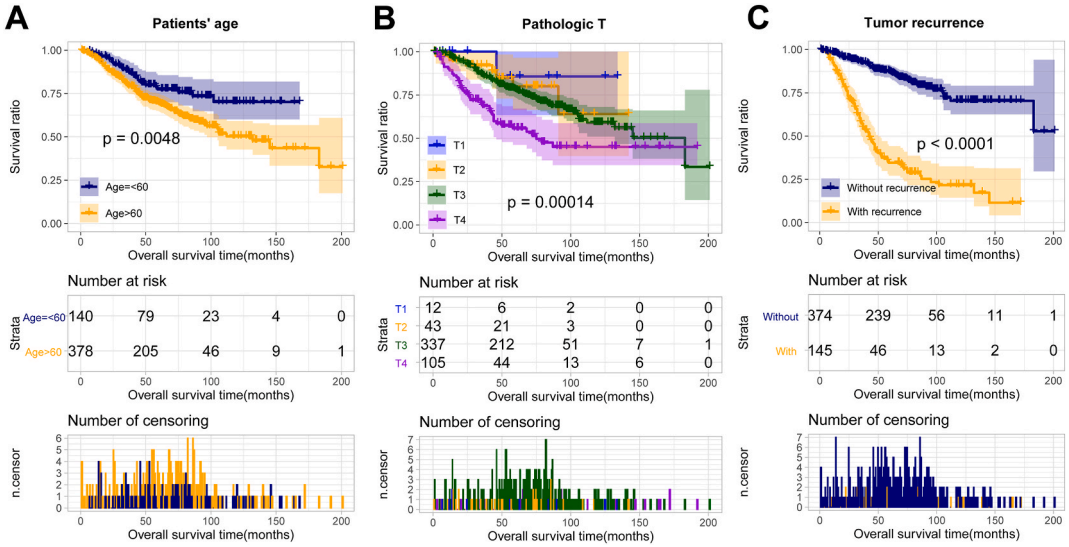

Fig. 7. Kaplan–Meier curve of age, pathologic T, and tumor recurrence in GSE39582 validation set. A: age; B: pathologic T; C: tumor recurrence.

3.5. The expression level of DEFGs in FS model between different risk groups

We further compared the expression levels of the four DEFGs in the FS model between the high- and low-risk groups in the TCGA training set and GSE39582 validation set. Compared with that in the low-risk group, the expression levels of *CYBB*, *ACSL4*, and *ACSL6* were significantly upregulated, whereas that of *PRNP* was evidently downregulated in the high-risk group ($P < 0.05$, Fig. 8A and B).

3.6. Combination of FS model and clinical factors shows the best prognostic performance

Altogether, we constructed multiple models, including four models based on four DEFGs in the FS model, the FS model, three models based on three independent clinical prognostic factors, a model based on a combination of these three clinical prognostic factors, and a model based on the combination of the FS model and clinical prognostic factors model. Subsequently, we compared model performance based on these factors using the ROC curve in the TCGA training set and GSE39582 validation set (Fig. 9). The results showed that the model based on the combination of the FS model and clinical factors had the best performance in both the TCGA training set (area under the curve [AUC] = 0.897, Fig. 9A) and the GSE39582 verification set (AUC = 0.858, Fig. 9B).

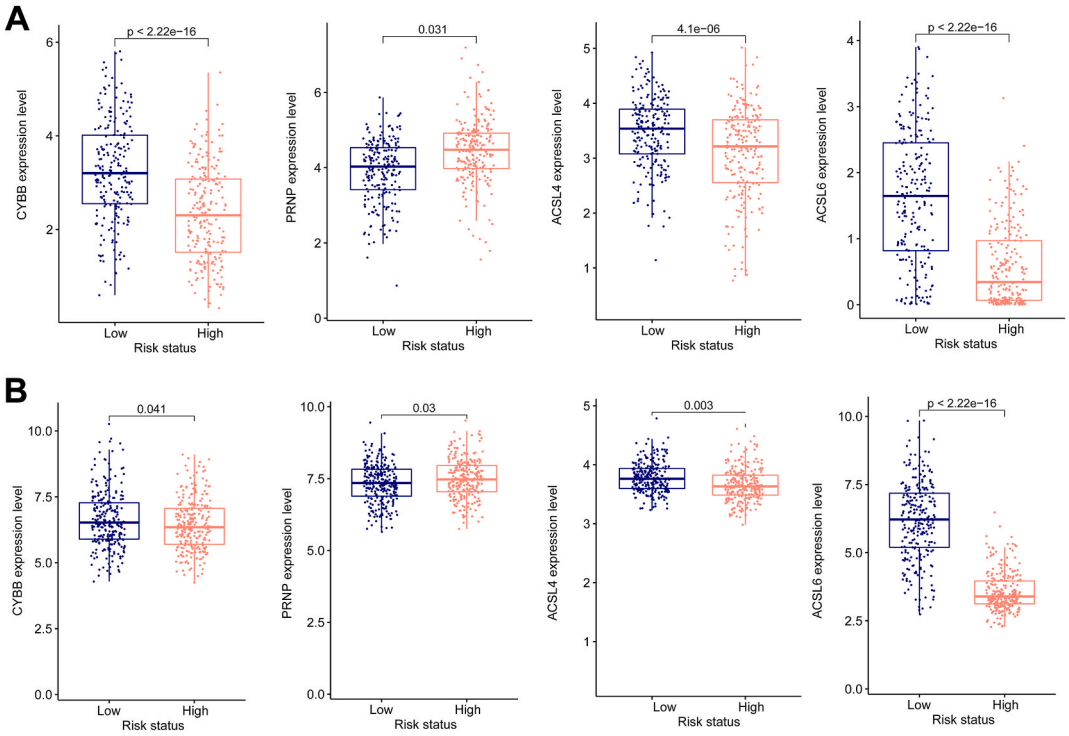

Fig. 8. Comparison of the expression levels of the four genes, including *CYBB*, *PRNP*, *ACSL4*, and *ACSL6* between high-risk group and low-risk group. A: TCGA training set; B: GSE39582 validation set. TCGA, The Cancer Genome Atlas.

4. Discussion

COAD is a highly malignant gastrointestinal tumor. In the clinic, prognosis assignment is important in therapeutic decision-making; therefore, it is vital to screen effective biomarkers for prognosis prediction. In the present study, 24 DEFGs in COAD were identified, four of which were involved in the prognostic signature of FS, including *CYBB*, *PRNP*, *ACSL4*, and *ACSL6*. Clinical characteristics, including age, pathological T stage, and tumor recurrence, were confirmed as independent prognostic factors. The FS model combined with the independent clinical prognostic factors showed the best prognostic ability, and the AUCs representing the predictive effect for the model were 0.897 and 0.858 in TCGA and GSE39582 datasets, respectively.

Four DEFGs were identified as prognostic biomarkers: *CYBB*, *PRNP*, *ACSL4*, and *ACSL6*. *CYBB* is the primary component of the microbicidal oxidase system in phagocytes. Boer et al. showed that aberrant *CYBB* mRNA splicing can result in primary immunodeficiency [22]. *PRNP* plays roles in iron uptake and iron homeostasis, and 11 unique disease-associated gene mutations have been discovered [23]. Furthermore, the prognostic implications of *PRNP* for the 3-year survival in colorectal cancer has been proposed by Anna et al. [24]. Until now, in humans and rodents, a total of five isoforms of *ACSL* have been investigated, namely *ACSL1*, *ACSL3*, *ACSL4*, *ACSL5*, and *ACSL6*, and their roles in fatty acid metabolism have been widely accepted. *ACSL4* dictates the sensitivity of ferroptosis by shaping the cellular lipid composition. Previous evidence has shown that this gene promotes the growth and invasion of prostate cancer [25]. The activation of *ACSL4* is critical in ferroptosis-induced intestinal ischemia/reperfusion injury [26]. *ACSL6* is found to be decreased in most forms of cancers and acts as a prognostic gene for CRC [27]. Altogether, we found relatively concentrated expression levels of the aforementioned four genes in the high- and low-risk groups, suggesting their prognostic role in COAD.

Clinical factors, including age, pathological T stage, and tumor recurrence, were identified as independent prognostic factors for COAD. Furthermore, Kaplan–Meier analysis revealed that patients aged less than 60 years, those with pathologic T1, and those having tumors without recurrence had better survival performance. These clinical factors have been previously reported as prognostic factors in various cancers [28,29]. For example, a retrospective cohort study designed by Laohavinij et al. demonstrated that patients with COAD aged more than 60 years old and those at stage III and IV had poorer survival performance [30].

A novel prognostic signature composed of the aforementioned four DEFGs was constructed to predict OS. As expected, compared with that in patients in the low-risk group, patients with high FS scores had significantly poorer OS. Recently, multiple ferroptosis-related gene signatures have been proposed to predict the clinical prognosis of various cancers [31,32]. In this study, we further constructed the model based on the FS model and the clinical prognostic factors, including age, pathologic T, and tumor recurrence, which showed better prognostic performance than that of the model constructed based on individual DEFG. Pub.

However, this study had some limitations. This study used bioinformatics tools to construct a ferroptosis-based prognostic signature according to data from publicly available databases; therefore, the potential prognostic ability should be verified in further prospective

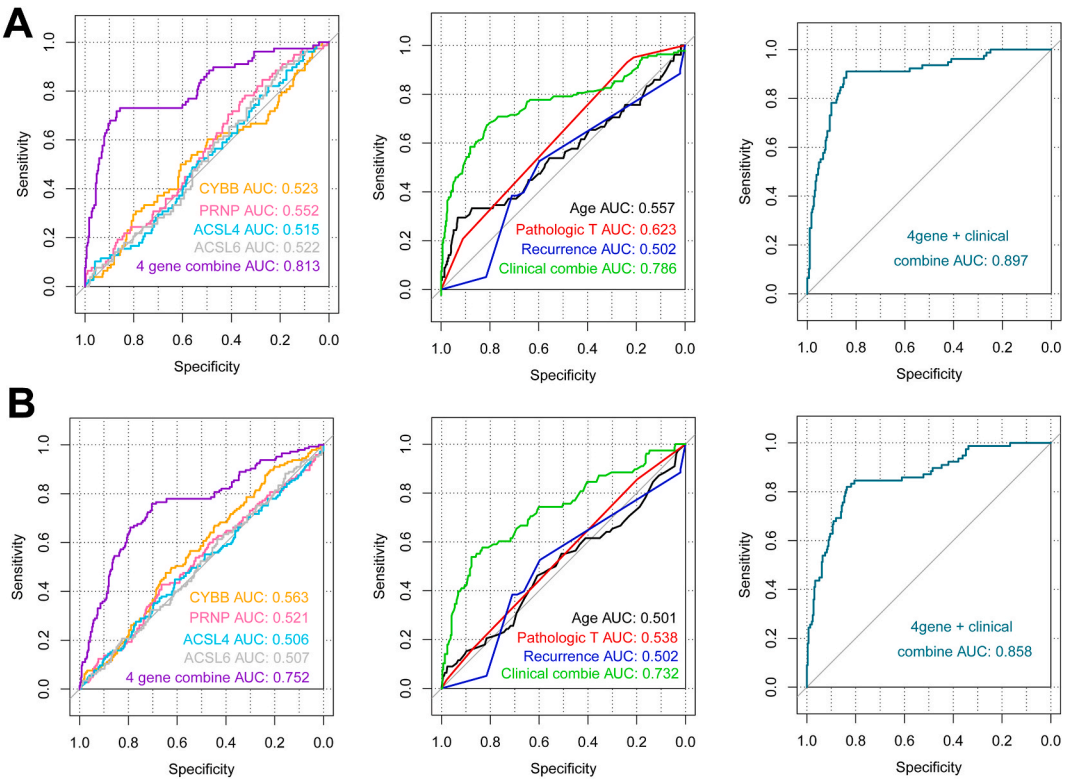

Fig. 9. Receiver operating characteristic (ROC) curve of multiple models in TCGA training set and GSE39582 validation set. A: TCGA training set; B: GSE39582 validation set. Left: ROC curve for the prognosis based on four important ferroptosis genes and the combination of the four ferroptosis genes; Middle: ROC curve for the prognosis based on three independent prognostic significant clinical factors and the combination of three independent prognostic clinical factors; Right: ROC curve based on the comprehensive prognosis model of FS model combined clinical factor model. TCGA, The Cancer Genome Atlas; FS, ferroptosis score.

trials with larger sample sizes. Furthermore, experiments *in vitro* and *in vivo* are required to verify our conclusions.

5. Conclusion

In conclusion, the ferroptosis-based signature combined with clinical prognostic factors showed promising clinical predictive value in COAD, which would be beneficial for personalized management of patients with COAD. Further investigation of this prognostic model is worthwhile for therapeutic decision-making.

Ethics approval and consent to participate

Not applicable.

Consent for publication

Not applicable.

Data availability statement

All data generated or analyzed during this study are included in this article. Further enquiries can be directed to the corresponding author.

Funding

None.

CRediT authorship contribution statement

Yicong Fang: Writing – original draft, Validation, Methodology, Investigation, Conceptualization. **Lin Han:** Writing – original draft, Methodology, Investigation, Formal analysis, Conceptualization. **Qiuxia Hong:** Validation, Software, Resources, Investigation, Data curation. **Guan-Cong Wang:** Validation, Resources, Methodology, Investigation, Data curation. **Xia-Juan Xue:** Software, Methodology, Investigation, Formal analysis. **Qunzhang Zeng:** Writing – review & editing, Supervision, Project administration, Funding acquisition, Conceptualization. **Jing Liu:** Writing – review & editing, Visualization, Supervision, Funding acquisition, Conceptualization.

Declaration of competing interest

The authors declare that they have no known competing financial interests or personal relationships that could have appeared to influence the work reported in this paper.

Acknowledgements

None.

List of abbreviations

colon adenocarcinoma (COAD)
the cancer genome atlas (TCGA)
Differtially expressed ferroptosis-related genes (DEFGs)
Ferroptosis score (FS)
overall survival (OS)
receiver operating characteristic (ROC)
colon adenocarcinoma (COAD)
reactive oxygen species (ROS)
differentially expressed ferroptosis-related genes (DEFGs)
ferroptosis score (FS)
least absolute shrinkage and selection operator (LASSO)
area under receiver operator characteristic (AUROC)

References

[1] R.L. Siegel, K.D. Miller, H.E. Fuchs, A. Jemal, Cancer statistics, 2021, CA A Cancer J. Clin. 71 (1) (2021) 7–33, https://doi.org/10.3322/caac.21654.
[2] W. Chen, R. Zheng, P.D. Baade, S. Zhang, H. Zeng, F. Bray, et al., Cancer statistics in China, 2015, CA A Cancer J. Clin. 66 (2) (2016) 115–132, https://doi.org/10.3322/caac.21338.
[3] V. Barresi, L. Reggiani Bonetti, A. Ieni, R.A. Caruso, G. Tuccari, Histological grading in colorectal cancer: new insights and perspectives, Histol. Histopathol. 30 (9) (2015) 1059–1067, https://doi.org/10.14670/HH-11-633.
[4] R.N. Berri, E.K. Abdalla, Curable metastatic colorectal cancer: recommended paradigms, Curr. Oncol. Rep. 11 (3) (2009) 200–208, https://doi.org/10.1007/s11912-009-0029-z.
[5] S. Pita-Fernandez, L. Gonzalez-Saez, B. Lopez-Calvino, T. Seoane-Pillado, E. Rodriguez-Camacho, A. Pazos-Sierra, et al., Effect of diagnostic delay on survival in patients with colorectal cancer: a retrospective cohort study, BMC Cancer 16 (2016) 664, https://doi.org/10.1186/s12885-016-2717-z.
[6] S.J. Dixon, Ferroptosis: bug or feature? Immunol. Rev. 277 (1) (2017) 150–157, https://doi.org/10.1111/imr.12533.
[7] B. Hassannia, P. Vandenabeele, T. Vanden Berghe, Targeting ferroptosis to iron out cancer, Cancer Cell 35 (6) (2019) 830–849, https://doi.org/10.1016/j.ccell.2019.04.002.
[8] T. Liu, H. Luo, J. Zhang, X. Hu, J. Zhang, Molecular identification of an immunity- and Ferroptosis-related gene signature in non-small cell lung Cancer, BMC Cancer 21 (1) (2021) 783, https://doi.org/10.1186/s12885-021-08541-w.
[9] N. Tao, K. Li, J. Liu, Molecular mechanisms of ferroptosis and its role in pulmonary disease, Oxid. Med. Cell. Longev. 2020 (2020) 9547127, https://doi.org/10.1155/2020/9547127.
[10] Y. Tang, C. Li, Y.J. Zhang, Z.H. Wu, Ferroptosis-Related Long Non-Coding RNA signature predicts the prognosis of Head and neck squamous cell carcinoma, Int. J. Biol. Sci. 17 (3) (2021) 702–711, https://doi.org/10.7150/ijbs.55552.
[11] X. Xu, X. Zhang, C. Wei, D. Zheng, X. Lu, Y. Yang, et al., Targeting SLC7A11 specifically suppresses the progression of colorectal cancer stem cells via inducing ferroptosis, Eur. J. Pharmaceut. Sci. 152 (2020) 105450, https://doi.org/10.1016/j.ejps.2020.105450.
[12] S. Park, J. Oh, M. Kim, E.J. Jin, Bromelain effectively suppresses Kras-mutant colorectal cancer by stimulating ferroptosis, Anim. Cell Syst. 22 (5) (2018) 334–340, https://doi.org/10.1080/19768354.2018.1512521.
[13] X. Qi, R. Wang, Y. Lin, D. Yan, J. Zuo, J. Chen, et al., A ferroptosis-related gene signature identified as a novel prognostic biomarker for colon cancer, Front. Genet. 12 (2021) 692426, https://doi.org/10.3389/fgene.2021.692426.
[14] R. Edgar, M. Domrachev, A.E. Lash, Gene Expression Omnibus: NCBI gene expression and hybridization array data repository, Nucleic Acids Res. 30 (1) (2002) 207–210, https://doi.org/10.1093/nar/30.1.207.
[15] L. Marisa, A. de Reynies, A. Duval, J. Selves, M.P. Gaub, L. Vescovo, et al., Gene expression classification of colon cancer into molecular subtypes: characterization, validation, and prognostic value, PLoS Med. 10 (5) (2013) e1001453, https://doi.org/10.1371/journal.pmed.1001453.
[16] J.Y. Liang, D.S. Wang, H.C. Lin, X.X. Chen, H. Yang, Y. Zheng, et al., A novel ferroptosis-related gene signature for overall survival prediction in patients with hepatocellular carcinoma, Int. J. Biol. Sci. 16 (13) (2020) 2430–2441, https://doi.org/10.7150/ijbs.45050.

[17] L. Wang, C. Cao, Q. Ma, Q. Zeng, H. Wang, Z. Cheng, et al., RNA-seq analyses of multiple meristems of soybean: novel and alternative transcripts, evolutionary and functional implications, BMC Plant Biol. 14 (2014) 169, https://doi.org/10.1186/1471-2229-14-169.
[18] X. Zhang, L. Ren, X. Yan, Y. Shan, L. Liu, J. Zhou, et al., Identification of immune-related lncRNAs in periodontitis reveals regulation network of gene-lncRNA-pathway-immunocyte, Int. Immunopharm. 84 (2020) 106600, https://doi.org/10.1016/j.intimp.2020.106600.
[19] P. Wang, Y. Wang, B. Hang, X. Zou, J.H. Mao, A novel gene expression-based prognostic scoring system to predict survival in gastric cancer, Oncotarget 7 (34) (2016) 55343–55351, https://doi.org/10.18632/oncotarget.10533.
[20] J.J. Goeman, L1 penalized estimation in the Cox proportional hazards model, Biometrical journal Biometrische Zeitschrift 52 (1) (2010) 70–84, https://doi.org/10.1002/bimj.200900028.
[21] X. Robin, N. Turck, A. Hainard, N. Tiberti, F. Lisacek, J.C. Sanchez, et al., pROC: an open-source package for R and S+ to analyze and compare ROC curves, BMC Bioinf. 12 (2011) 77, https://doi.org/10.1186/1471-2105-12-77.
[22] M. de Boer, K. van Leeuwen, J. Geissler, C.M. Weemaes, T.K. van den Berg, T.W. Kuijpers, et al., Primary immunodeficiency caused by an exonized retroposed gene copy inserted in the CYBB gene, Hum. Mutat. 35 (4) (2014) 486–496, https://doi.org/10.1002/humu.22519.
[23] S.B. Prusiner, K.K. Hsiao, Human prion diseases, Ann. Neurol. 35 (4) (1994) 385–395, https://doi.org/10.1002/ana.410350404.
[24] A.G. Antonacopoulou, P.D. Grivas, L. Skarlas, M. Kalofonos, C.D. Scopa, H.P. Kalofonos, POLR2F, ATP6V0A1 and PRNP expression in colorectal cancer: new molecules with prognostic significance? Anticancer Res. 28 (2B) (2008) 1221–1227.
[25] X. Wu, F. Deng, Y. Li, G. Daniels, X. Du, Q. Ren, et al., ACSL4 promotes prostate cancer growth, invasion and hormonal resistance, Oncotarget 6 (42) (2015) 44849–44863, https://doi.org/10.18632/oncotarget.6438.
[26] Y. Li, D. Feng, Z. Wang, Y. Zhao, R. Sun, D. Tian, et al., Ischemia-induced ACSL4 activation contributes to ferroptosis-mediated tissue injury in intestinal ischemia/reperfusion, Cell Death Differ. 26 (11) (2019) 2284–2299, https://doi.org/10.1038/s41418-019-0299-4.
[27] Z. Huang, Q. Yang, Z. Huang, Identification of critical genes and five prognostic biomarkers associated with colorectal cancer, Med. Sci. Mon. Int. Med. J. Exp. Clin. Res. 24 (2018) 4625–4633, https://doi.org/10.12659/MSM.907224.
[28] A.J. Nixon, D. Neuberg, D.F. Hayes, R. Gelman, J.L. Connolly, S. Schnitt, et al., Relationship of patient age to pathologic features of the tumor and prognosis for patients with stage I or II breast cancer, J. Clin. Oncol. 12 (5) (1994) 888–894, https://doi.org/10.1200/JCO.1994.12.5.888.
[29] P. Miccoli, M.N. Minuto, C. Ugolini, E. Panicucci, M. Massi, P. Berti, et al., Papillary thyroid cancer: pathological parameters as prognostic factors in different classes of age, Otolaryngol. Head Neck Surg. 138 (2) (2008) 200–203, https://doi.org/10.1016/j.otohns.2007.10.034.
[30] S. Laohavinij, J. Maneechavakajorn, P. Techatanol, Prognostic factors for survival in colorectal cancer patients, J. Med. Assoc. Thai. 93 (10) (2010) 1156–1166.
[31] Y. Hong, M. Lin, D. Ou, Z. Huang, P. Shen, A novel ferroptosis-related 12-gene signature predicts clinical prognosis and reveals immune relevancy in clear cell renal cell carcinoma, BMC Cancer 21 (1) (2021) 831, https://doi.org/10.1186/s12885-021-08559-0.
[32] F. Xu, Z. Zhang, Y. Zhao, Y. Zhou, H. Pei, L. Bai, Bioinformatic mining and validation of the effects of ferroptosis regulators on the prognosis and progression of pancreatic adenocarcinoma, Gene 795 (2021) 145804, https://doi.org/10.1016/j.gene.2021.145804.